

Article

# Study on the mechanical properties of biomolecules in watershed water resource management

Zairan Li<sup>1</sup>, Na Fu<sup>2,\*</sup><sup>1</sup> College of Hydraulic Science and Engineering, Yangzhou University, Yangzhou 225009, China<sup>2</sup> Editorial Department of Journal, Yangzhou University, Yangzhou 225009, China\* **Corresponding author:** Na Fu, [yzufun@163.com](mailto:yzufun@163.com)

## CITATION

Li Z, Fu N. Study on the mechanical properties of biomolecules in watershed water resource management. *Molecular & Cellular Biomechanics*. 2025; 22(2): 695. <https://doi.org/10.62617/mcb695>

## ARTICLE INFO

Received: 1 November 2024

Accepted: 11 November 2024

Available online: 10 February 2025

## COPYRIGHT



Copyright © 2025 by author(s).

*Molecular & Cellular Biomechanics* is published by Sin-Chn Scientific Press Pte. Ltd. This work is licensed under the Creative Commons Attribution (CC BY) license.

<https://creativecommons.org/licenses/by/4.0/>

**Abstract:** This study focuses on the mechanical properties of biomolecules and their interactions within the extracellular matrix in the context of watershed water resource management. We utilized a modified WEAP-MODFLOW model to explore how these interactions influence the allocation and management of water resources. The WEAP model serves as a comprehensive tool for assessing the balance of surface water supply and demand, while the MODFLOW model is employed for simulating deep groundwater flow. By integrating these models, we can examine the mechanical behavior of biomolecules and cells in response to varying hydrological conditions, thus enhancing our understanding of their role in water resource dynamics. To improve model accuracy, parameters were calibrated using observed flow data from relevant biological systems. Key evaluation metrics, including the coefficient of determination, Nash efficiency coefficient, and deviation coefficient, were employed to assess simulation accuracy. On a monthly scale, the coefficient of determination reached 0.98, indicating a strong correlation between simulated and observed values. The Nash efficiency coefficient was 0.97, reflecting high accuracy in simulating flow dynamics. Furthermore, a deviation coefficient of -12% suggests minimal systematic bias in the simulation results. During the validation phase, these metrics maintained high accuracy, with a determination coefficient of 0.97, a Nash efficiency coefficient of 0.97, and a deviation coefficient of -3.30%. These findings highlight the reliability of the improved WEAP-MODFLOW model in simulating the mechanical properties of biomolecules and their interactions with water resources, ultimately contributing to optimized water resource management strategies.

**Keywords:** mechanical properties; biomolecules; extracellular matrix; water resource management; coupled models

## 1. Introduction

By constructing WEAP and MODFLOW modified models and realizing the differential coupling between the improved models using LinkKitchen software, the combined utilization of surface water and deep groundwater is optimized [1,2]. The refined model's parameters were optimized using measured flow data, and its accuracy was evaluated with R<sup>2</sup>, NSE (Nash-Sutcliffe Efficiency), and PBIAS (Percent bias) [3,4]. Results demonstrate that the WEAP-MODFLOW differential coupling model accurately simulates water supply and demand in the region [5]. The Budyko theory, rooted in the principle of differential coupling equilibrium, was developed by a Soviet climatologist focused on the global balance between water and energy [6,7]. This theory has since become instrumental in the fields of hydrology and climatology for examining natural evaporation processes over land surfaces that

cannot be controlled by humans. According to Budyko, long-term evaporation aligns with the availability of atmospheric water and the ecosystem's evaporation capacity. A core aspect of the theory is the hydrothermal coupling hypothesis, which assumes that water and energy in a watershed reach equilibrium over extended periods [8]. This approach posits that actual basin evaporation results from a balance between precipitation and potential evaporation [9]. Budyko's equation, combining these water and energy relationships, calculates actual evaporation based on precipitation and potential evaporation inputs, effectively modeling evaporation trends within watersheds [10,11].

The Budyko curve illustrates this balance, showing how evaporation patterns respond to the interaction between precipitation and evaporation potential in diverse watersheds [12]. Building on this theory, the elasticity coefficient method emerged to assess how sensitive runoff is to variations in precipitation and potential evapotranspiration [13]. This method provides a tool for analyzing runoff changes driven by climate shifts by examining fluctuations in precipitation and evaporation potential. Through differential coupling equations, this approach computes sensitivity coefficients that quantify runoff's response to changing climate variables, offering valuable insights into the resilience or vulnerability of water systems under climate change [14,15]. This paper delves into quantifying the impact of benign human activities on runoff variations. We isolate the runoff change attributed to human activities by isolating climate change's influence. This approach clarifies their roles, aiding watershed management and water resources planning [16,17]. We developed the WEAP-MODFLOW coupled model for optimal water allocation, integrating surface water-deep groundwater simulation. WEAP assesses surface water supply demand, consumption, and quality, while MODFLOW simulates deep groundwater flow and management, enhancing resource optimization. Through the differential coupling of the LinkKitchen software, the two, improved models can work together to achieve a joint simulation of surface water and deep groundwater [18,19].

## 2. Related algorithm of water resources optimal allocation

### 2.1. Optimal allocation of water resources based on multi-objective planning

Multi-objective optimization is a significant area in mathematical programming, developed to address the challenge of optimizing multiple objectives within a defined region. This approach is essential for real-world applications, where achieving the best outcomes often involves balancing competing priorities. In contexts requiring complex decision-making, as illustrated in Equations (1) and (2), multiple conflicting objectives must frequently be evaluated and optimized simultaneously.

$$ET_0 = \frac{0.408\Delta(R_n - G) + \gamma \frac{900}{T + 273} U_2(e_s - e_a)}{\Delta + \gamma(l + 0.34U_2)} + Yu(f, x) \quad (1)$$

$$ET_c = ET_0 \times K_c \div FC - F(g, x) \quad (2)$$

In water resources management, this paper will need to balance multiple objectives such as ensuring water supply, security, economic benefits and environmental protection. The solution for Mult objective optimization is usually not a single solution but a solution set called the Pareto optimal set. Pareto Solutions in the optimal set are called non-inferior solutions, as shown in Equation (3), when these solutions become better on one target, they must become worse on the other target.

$$K_c = K_{c(FAO)} + 0.04(U_2 - 2) - 0.04(RH_{min} - 45)\left(\frac{h}{3}\right)^{0.3} \quad (3)$$

Through graphical methods, the non-inferiority of Pareto optimal centralized solution can be intuitively displayed, so as to provide multiple optimization solutions for decision makers to choose the solution that most meets the actual requirements. As shown in Equation (4).

$$W_0 = ET_C - P_e \quad (4)$$

As shown in Equations (5) and (6), each solution in the Pareto optimal set is an optimal solution under a certain trade-off, so that no solution can surpass the other solution simultaneously on all targets.

$$W_C = (ET_C - P_e) \times S_C \times 10^{-4} \quad (5)$$

$$P_e = P - R_e \quad (6)$$

Through computational and graphical analysis, this paper will be able to obtain the Pareto optimal set and show the trade-off of the solution on each target. As shown in Equations (7) and (8).

$$WI_t = \sum_{i=1}^n (IGDP_{i,t} \times IWG_{i,t}) \quad (7)$$

$$W_i = S_i \times h_1 + Q_i \times h_2 \quad (8)$$

As shown in Equations (9) and (10), non-negative constraint means that the allocated water quantity of each water use department in each calculation partition shall be greater than 0.

$$y = ax_i + b \quad (9)$$

$$v_i = \frac{\sum_{i=1}^n v_i \frac{1}{d_i^k}}{\sum_{i=1}^n \frac{1}{d_i^k}}, i = 1, 2, \dots, n \quad (10)$$

## 2.2. Multi-objective optimization algorithm based on the genetic algorithm

As shown in Equations (11) and (12), the total water supply constraint means that the allocated water quantity of each calculation division shall not exceed the total water supply of the water supply department of each calculation division.

$$pdf(x) = \int_a^b f(x)dx \quad (11)$$

$$cdf(x) = \int_0^{x_p} pdf(x)dx \quad (12)$$

As shown in Equation (13), The goal of the improved model is to maximize the efficiency and economic benefits while meeting the constraints. Specifically, the constraints of the improved model include the total water demand, total water supply and non-negative constraints.

$$\rho_{XY|Z} = cov(\hat{\epsilon}, \hat{\zeta}) = \frac{cov(\hat{\epsilon}, \hat{\zeta})}{\sqrt{var(\hat{\epsilon})}\sqrt{var(\hat{\zeta})}} \quad (13)$$

As shown in Equation (14), the total amount of water demand constraint means that the water supply of each water supply source to each water use department shall not exceed the water demand of the water use department.

$$\frac{E}{P} = 1 + \frac{E_0}{P} - [1 + (\frac{E_0}{P})^\omega]^{\frac{1}{\omega}} \quad (14)$$

As shown in Equations (15) and (16), Through the total amount of water demand, we can ensure that the water obtained by each water department matches its actual demand, and improve the utilization efficiency of water resources.

$$ET_0 = \frac{0.408\Delta(R_n - G) + \gamma \frac{900}{T_{mean} + 273} u_2(e_s - e_a)}{\Delta + \gamma(1 + 0.34u_2)} \quad (15)$$

$$\frac{\partial}{\partial x} (k_{xx} \frac{\partial h}{\partial x}) + \frac{\partial}{\partial y} (k_{yy} \frac{\partial h}{\partial y}) + \frac{\partial}{\partial z} (k_{zz} \frac{\partial h}{\partial z}) + w = S_s \quad (16)$$

This constraint ensures that the water supply of the water supply sector is not overdistributed throughout the study area, as shown in Equations (17) and (18), thereby maintaining the stability of the water supply system.

$$h(x, y, z, t)|_{t=0} = h_0(x, y, z) \quad (17)$$

$$k_n \frac{\partial h}{\partial n} |_{S_2} = q(x, y, z, t) \quad (18)$$

The total water supply of the reservoir in an area is limited, and the water supply capacity of the water supply constraints, as shown in Equations (19) and (20), to ensure the safe operation of the water supply system.

$$\frac{\partial}{\partial x} [K(H - Z) \frac{\partial H}{\partial x}] + \frac{\partial}{\partial y} [K(H - Z) \frac{\partial H}{\partial y}] + \omega + Q = \mu \quad (19)$$

$$NSE = 1 - \frac{\sum_{i=1}^n (Q_{obs,i} - Q_{sim,i})^2}{\sum_{i=1}^n (Q_{obs,i} - \overline{Q_{obs}})^2} \quad (20)$$

### 3. A improved model based on differential coupling equilibrium

#### 3.1. Improvement model design of the unsettled river basin based on the hydrothermal differential coupling equilibrium assumption

Vertical decomposition method is a watershed analysis method based on the assumption of differential coupling equilibrium [20,21]. Because of its simple principle and strong physical properties. This method is mainly used to quantitatively distinguish the climate change from the benign human activities, and the influence of evapo uncontrollable emission or runoff in the river basin [22,23]. The analysis of variation points in evapotranspiration or runoff time series allows researchers to divide the sequence into distinct stages, enabling attribution of changes to specific factors. However, most existing studies focus on annual averages, leaving shorter time scales relatively underexplored [24,25]. The vertical decomposition method, grounded in the differential hydrothermal coupling equilibrium theory, proposes that climate and beneficial human activities are key drivers of basin hydrology [26]. This approach partitions time series into stages that reflect distinct climatic conditions or intensities of human influence by identifying variation points in watershed evapotranspiration and runoff [27,28]. The analysis involves gathering comprehensive long-term data, preprocessing to ensure accuracy, and employing statistical techniques to detect these variation points, which serve as indicators of climate fluctuations or anthropogenic impacts [29,30]. By delineating stages associated with particular climate events or human activities, quantitative analysis can then measure each factor’s contribution to changes in evapotranspiration or runoff at different stages, providing insights into the specific influences shaping basin hydrology. **Figure 1** shows the flow chart of the hydrological cycle process simulation algorithm. In the design of the improved model of the Wuding River basin, the vertical decomposition method is used to quantitatively distinguish climate change from benign human activities, and affect the effects of uncontrollable steam emission and runoff in the basin. Wuding River basin is located in the northwest of China and is a typical semi-arid region, and climate change and benign human activities have a significant impact on water resources. Therefore, constructing a hydrological improvement model that can accurately reflect the effects of climate change and benign human activities is of great significance for watershed management and optimal allocation of water resources.

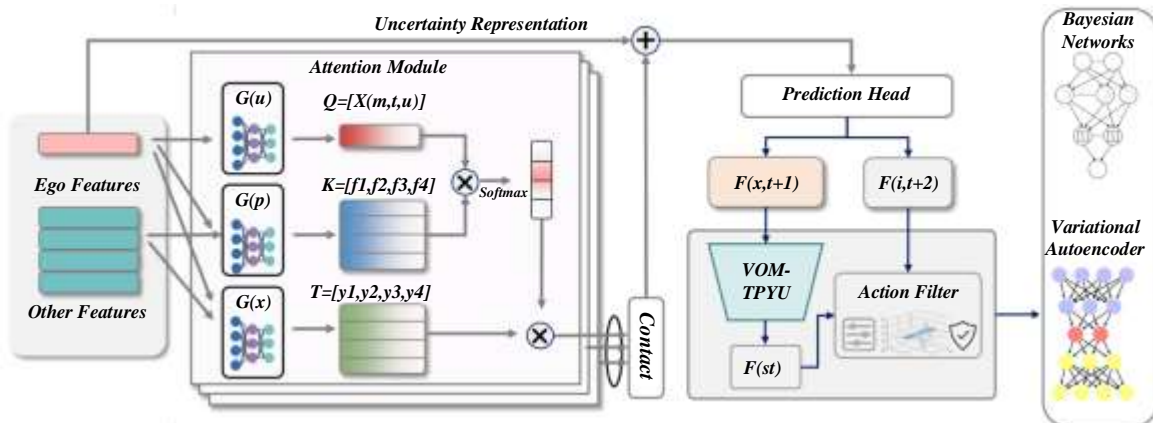


**Figure 1.** Flow chart of the simulation algorithm of the hydrological cycle process.

Collection of climate controllable data and hydrological controllable data: the climate controllable data of Wuding River basin includes precipitation, temperature and steam, uncontrollable distribution of controllable data, and hydrological controllable data include runoff and water level controllable data. The primary sources of controllable data consist of long-term observational records collected from meteorological and hydrological monitoring stations. To identify variation points in uncontrollable evapotranspiration and runoff sequences, the vertical decomposition method is employed, allowing the complete time series to be segmented into various stages. Each segment represents the effects of specific climatic conditions or beneficial human interventions on the watershed. By examining the mean changes in uncontrollable emissions and runoff across these stages, we can quantitatively assess the contributions of climate change and positive human activities to the watershed's water resources. To enhance the accuracy and reliability of the modified model, it was validated and fine-tuned using measured controllable data from diverse regions within the basin. By comparing simulation outcomes with the observed controllable data, we ensure that the enhanced model accurately reflects the impacts of climate change and beneficial human activities on the hydrological dynamics of the Wuding River basin. While the vertical decomposition method is frequently applied to annual averages, its effectiveness diminishes in shorter time frames. **Figure 2** illustrates the optimized configuration of the multi-objective genetic algorithm. In regions with pronounced seasonal fluctuations, this method may fail to effectively capture the immediate impacts of climate change and human activities. Thus, improving the temporal resolution and analytical precision of the modified model is essential, potentially through the integration of additional time series analysis techniques such as sliding averages and Fourier transforms.

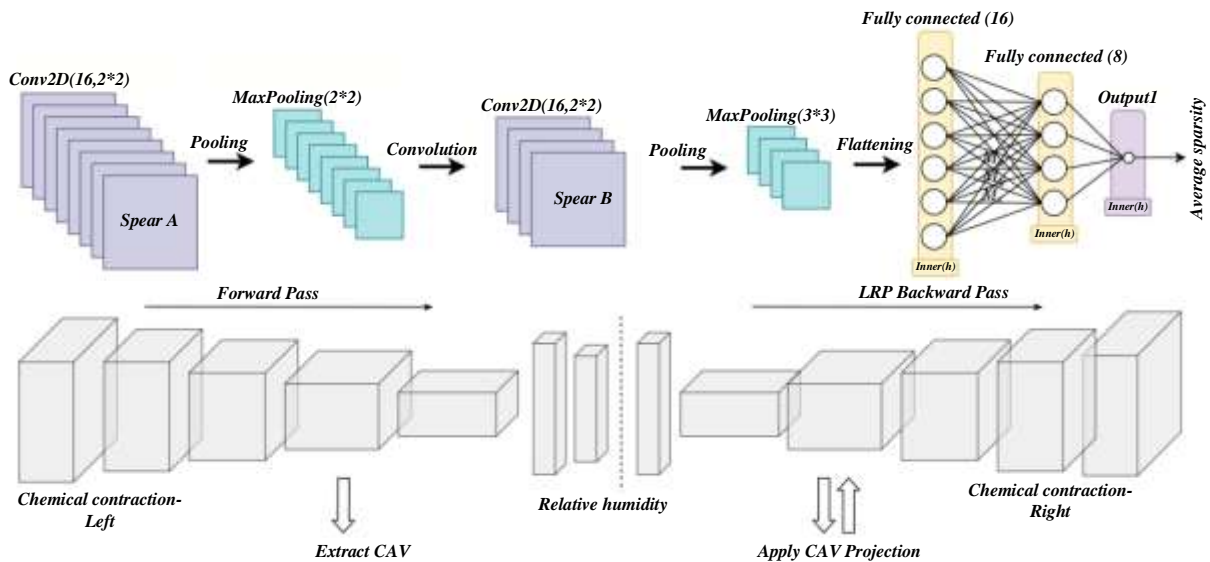


**Figure 2.** Optimization configuration diagram of the multi-target genetic algorithm.

### 3.2. Exploration of the driving mechanism of watershed evapotranspiration based on the assumption of Budyko differential coupling equilibrium

The hypothesis of differential hydrothermal coupling equilibrium was introduced by Budyko, a renowned climatologist from the former Soviet Union, during his investigation of global water quantity and energy balance. He discovered that the long-term average capacity for uncontrollable evapotranspiration from land is primarily influenced by the balance between atmospheric water supply and the land's capacity for uncontrollable emissions. Building on this foundational idea, Budyko formulated a hydrothermal differential coupled equilibrium equation, enabling the calculation of actual uncontrollable emissions based on precipitation and evaporation capacities. Initially, this hypothesis did not account for basin-specific characteristics; however, as research progressed, numerous scholars calibrated the empirical relationships governing hydrothermal balance in various basins using observed meteorological and runoff data. These studies validated Budyko's hypothesis and introduced distinct empirical formulas that incorporate underlying surface factors. Such formulas consider characteristics like vegetation cover, soil type, and land use, allowing for a more accurate depiction of the mechanisms driving uncontrollable evaporation in watersheds. **Figure 3** illustrates the assessment of average annual precipitation across the basin. Both climate change and beneficial human interventions significantly influence the actual distribution of uncontrollable evapotranspiration, subsequently affecting runoff at the basin's outlet through water balance dynamics. The impacts of climate change encompass alterations in precipitation patterns and temperature variations, while the effects of positive human activities include changes in land use, irrigation practices, urbanization, and the development of water resources. These factors collectively contribute to the complexities of hydrological processes within the watershed. Based on the Budyko hydrothermal equilibrium hypothesis, the effects of climate change and benign human activities on the actual uncontrollable emission volume of the watershed can be quantitatively distinguished, so as to calculate the effects of the two on runoff.

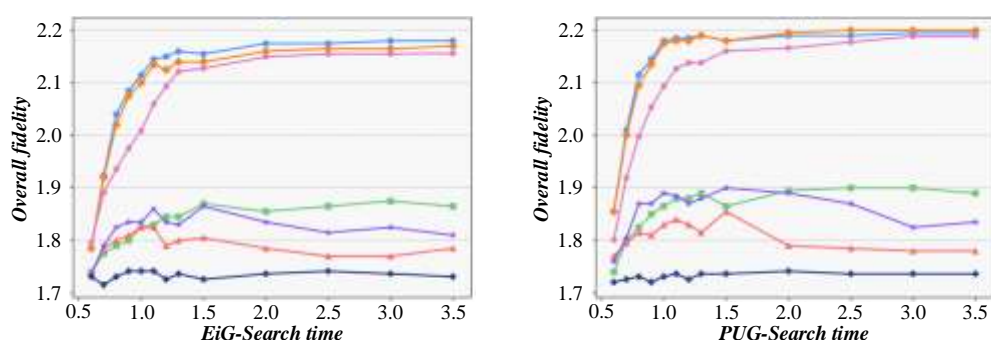


**Figure 3.** Assessment chart of the average annual precipitation in the river basin.

By comparing the uncontrollable steam emission and runoff changes under different land use methods, the utilization efficiency of water resources in agricultural, urban and natural areas can be determined. Combined with the comprehensive controllable data of climate change and benign human activities, the Budyko

hypothesis was used to establish a water balance improvement model to assess the comprehensive impact. In a rapidly urbanized area, improved model simulation can predict the combined impact of future climate change and benign human activities on water resources in the basin, so as to provide scientific basis for water resources management. In practical application, based on Budyko, the hypothesis of the uncontrollable emission driving mechanism of watershed steaming has achieved remarkable results. For example, in the study of a certain watershed, by analyzing long time series of meteorological and runoff controllable data, the Budyko hypothesis quantitatively distinguishes between climate change and human benign activities on the uncontrollable distribution of the watershed. The results show that climate change mainly affects the uncontrollable emission and quantity through the decrease of precipitation and rising temperature, while the benign human activities mainly affect the uncontrollable emission of evaporation through the increase of land use change and irrigation. **Figure 4** shows the trend assessment chart of seasonal runoff changes, which predicts the change trend of water resources under different climate scenarios in the future, and provides an important reference for watershed water resources management.

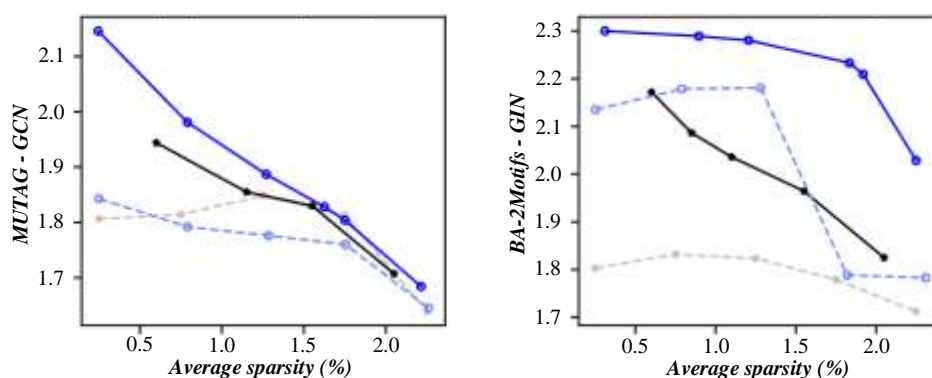


**Figure 4.** Evaluation diagram of seasonal runoff change trends.

#### 4. Study on optimal allocation of water resources in river basin based on improved improvement model

Due to its solid physical foundation and strong operability, Budyko has been widely used in recent years in the quantitative analysis of the effects of climate change and benign human activities. The specific applications include the following aspects: By comparing the controllable data of precipitation and evaporation in different periods, the impact of climate change on evaporation emission and runoff can be evaluated. For example, in a long-term observed watershed, analyzing the change trend of uncontrollable emission and runoff before and after climate change can determine the impact of climate change on water resources. Using controllable data such as land use change, irrigation volume and urbanization, we can assess the impact of benign human activities on water resources in the river basin. The verification process is mainly divided into the following steps: Collect and organize the controllable data of deep groundwater level observation measured in the field to ensure that the spatial and temporal distribution of controllable data is consistent with the scope covered by the improved model. **Figure 5** shows the dynamic assessment

diagram of the reservoir, defining the upper and lower limits of the observed value. The calculation of the error values can be determined by measuring the difference between the controllable data and the simulation results of the modified model.

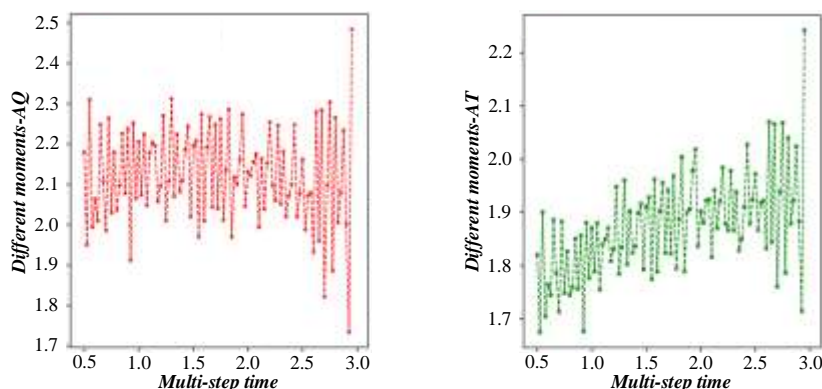


**Figure 5.** Dynamic assessment diagram of reservoir storage capacity.

The error value distribution is depicted using color-coded plots and other visual aids. In real-world scenarios, assessing and confirming deep groundwater models often requires advanced simulation software specifically designed for groundwater analysis. This software constructs a three-dimensional model of groundwater flow by incorporating geological data and hydrological information, allowing for numerical simulations that reflect changes in groundwater levels and flow dynamics. The groundwater simulation software develops a 3D model while factoring in the distribution of geological layers, hydrological characteristics, and boundary conditions. To create an improved model, accurate geological data and hydrogeological parameters must be inputted. Using actual measurements of groundwater levels, adjustments to the model parameters are made through a function that determines the parameter rates, aiming for the simulation results to closely match the observed data. **Table 1** outlines the allocation plan for water resources based on the optimal comprehensive benefits strategy and evaluates the improved model’s accuracy and reliability by comparing simulated results with observed data. The refined simulation outcomes can illustrate the time-dependent changes in deep groundwater levels, thereby providing a robust scientific basis for subsequent water resource management and strategic decision-making. The identification and validation of deep groundwater improvement models is an important tool for water resource management and sustainable development. Through effective numerical simulation and accurate verification process, it can improve the understanding and management ability of deep groundwater resources, and provide technical support for ensuring the sustainable utilization of deep groundwater resources.

**Table 1.** Optimal comprehensive benefit scheme of water resources allocation.

A Particular Year	Life	Water Allocation	Agriculture	Industry	Animal Husbandry	Total Water Consumption
2025	4.72	1.786	16.7452	1.2458	0.8936	3.5374
2030	4.65	1.245	15.8712	1.7598	0.2726	4.1476
2035	4	1.45	150	1.5	0.08	3.9

In water resource management and planning, the model is established to consider the interaction of surface water and deep groundwater system, so as to more accurately simulate and predict the supply and demand of water resources. In this paper, we will discuss how the differential coupling improvement models based on WEAP (Water Evaluation and Planning System) and MODFLOW (Modular Three - Dimensional Finite - Difference Groundwater Flow Model) are evaluated and calibrated to ensure the accuracy and reliability of their simulation results. LinkKitchen As a key tool for connecting the WEAP and MODFLOW modified models, it is necessary to ensure the consistency of the two modified models at temporal and spatial scales. On time scales, the time steps of WEAP and MODFLOW need to be consistent, so that the calculated results of the improved models in different time periods can be effectively interacted and compared. At the spatial scale, LinkKitchen divides the grid distribution one by one according to the grid distribution of MODFLOW, and maps the catchment area, rivers, deep groundwater nodes and other elements in the WEAP improved model to the linked files. **Figure 6** shows the assessment map of agricultural irrigation water demand, which ensures the controllable data transmission and exchange of the improved model in different spatial units, including regional precipitation, field irrigation infiltration, river flow and surface runoff. These controllable data will affect the calculation of deep groundwater in the MODFLOW modified model. After the modified model is established, it is necessary to determine the parameters of the WEAP-MODFLOW differential coupling modified model first.

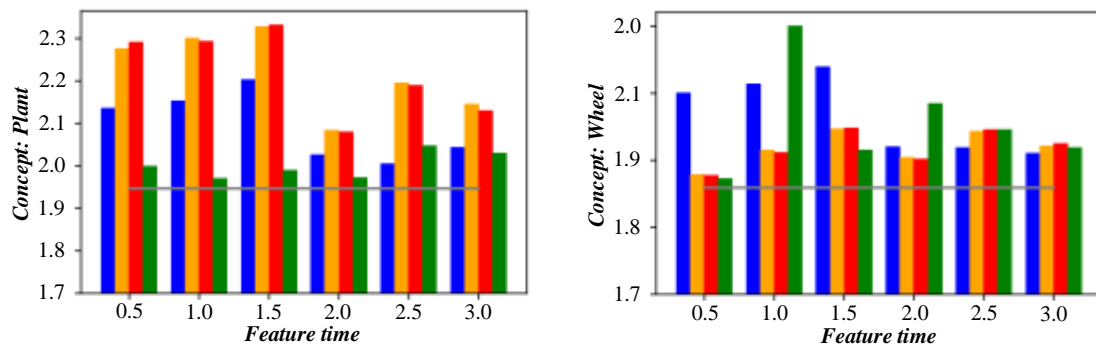


**Figure 6.** Assessment diagram of agricultural irrigation water demand.

The primary objective of the parameter adjustment process is to fine-tune various parameters within the enhanced model, ensuring that the simulation outputs align closely with the actual observed controllable data. Key parameters typically include those related to hydrogeological characteristics, hydrological processes, and boundary conditions of the improved model. By juxtaposing the simulation outcomes with empirical controllable data, we can identify the optimal combination of parameters. Validating the modified model is essential for assessing both its simulation accuracy and reliability. This validation involves comparing the model-generated controllable data—such as groundwater levels and surface runoff—with the actual measured data to evaluate simulation accuracy effectively. Historical data is also leveraged to test the model's predictive capabilities across various scenarios, including drought conditions and extreme precipitation events. Commonly employed evaluation metrics, such as the coefficient of determination, Nash efficiency coefficient, and deviation coefficient,

serve to objectively quantify how well the improved model's simulations correspond with the measured data. Sensitivity analysis further allows for the examination of how variations in different input parameters affect the model's output, thereby pinpointing which parameters significantly influence results. This analysis aids in the further refinement of the parameter settings within the modified model. Following this rigorous evaluation and calibration process, a precise and dependable WEAP-MODFLOW differential coupling improvement model can be established. This model is invaluable for exploring water resource supply and demand allocation and achieving optimal balances across diverse scenarios. **Table 2** presents the evaluation outcomes based on comprehensive benefit objectives. Additionally, this enhanced model is capable of performing historical simulations with existing data and forecasting future scenarios to inform strategic planning. For example, the impact of different water management strategies on watershed water systems can be simulated to support decision-making on sustainable water management. The process of establishment, evaluation and calibration of WEAP-MODFLOW differential coupling improvement model is a systematic engineering that needs to comprehensively consider the spatiotemporal consistency of the improved model, the parameter accuracy and the reliability of the simulation results.

**Table 2.** Evaluation results based on the comprehensive benefit objective.

Metric	2019	2020~2030	2019	2020~2030
Domestic Water Quota for Urban Residents (L/Person·d)	78	47	32	61
Water Consumption Quota for Rural Residents (L/Person·d)	96	64	40	72
Effective Utilization Coefficient of Farmland Irrigation Water	0.85	0.89	0.725	0.658
Water Supply Pipe Network Loss Rate (%)	10.32	7.42	1.1	15.3

## 5. Experimental analysis

The algorithm can find the best compromise by simulating natural selection and genetic variation processes between multiple targets. In this study, agricultural water distribution was considered as a rigid constraint for water resources. **Figure 7** shows the evaluation diagram of industrial water efficiency, optimizing the planting structure in the study area using NSGA-in the multi-objective genetic framework Pymoo. NSGA-is a commonly used multi-objective optimization algorithm with good global search capability and fast convergence performance, suitable for complex agricultural production optimization problems.

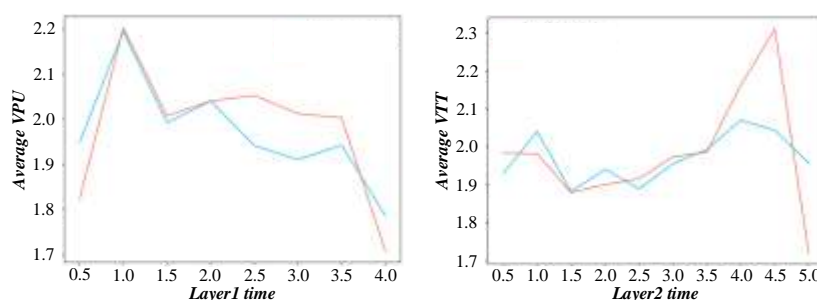


**Figure 7.** Assessment diagram of industrial water use efficiency.

This means that in the optimization process, this paper will have to ensure that the optimized planting structure can meet the needs of agricultural production under the existing water resources conditions, while not exceeding the total amount of available water resources. **Figure 8** shows the assessment map of urban water supply stability. This paper collects the controllable data of water resource supply and demand, agricultural water use efficiency and water demand of various crops in the research area in detail as the input parameters of the optimization and improvement model.

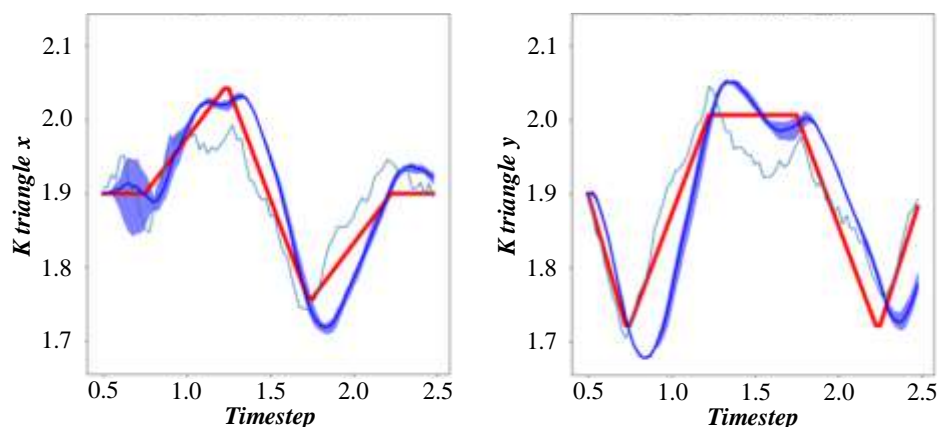


**Figure 8.** Assessment diagram of urban water supply stability.

The implementation of an optimized cropping structure has led to a notable enhancement in the efficiency of water resource utilization within the study area. In recent planning periods, the allocation of cultivated land for major crops has achieved a relatively equitable distribution, which not only ensures food security but also boosts the proportion of cash crops, thereby enhancing the economic returns of agricultural activities. As depicted in **Figure 9**, the assessment of ecological flow security levels indicates that, over the long-term planning horizon, advancements in water resource management technologies and improvements in agricultural productivity have facilitated further optimization of crop cultivation areas. This is particularly true for high-value crops such as grapes, goji berries, and apples, whose cultivation areas have expanded. This shift not only contributes to increased income for farmers but also supports the sustainable development of agricultural practices. By strategically adjusting the planting structure, the research highlights the dual benefits of enhancing water efficiency and promoting economic viability in agriculture, ultimately fostering a more resilient agricultural sector. The focus on cash crops reflects a proactive approach to maximizing economic benefits while maintaining essential food production. The positive outcomes associated with this optimized planting strategy underscore its importance in the broader context of water resource management and agricultural sustainability, reinforcing the necessity of adopting innovative practices that can adapt to changing environmental conditions. This approach not only addresses immediate agricultural needs but also aligns with long-term sustainability goals, ensuring that water resources are managed effectively to support both current and future generations.

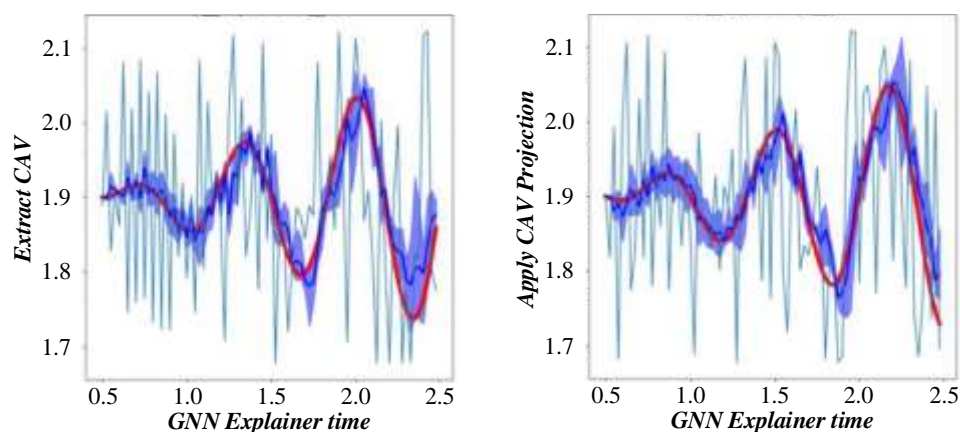


**Figure 9.** Assessment diagram of ecological flow guarantee level.

This paper will mainly focus on the afforestation benign activities, the influence of the basin steam uncontrollable distribution, especially in the calculation of afforestation water to the river basin steam uncontrollable contribution, only consider the steam uncontrollable distribution caused by afforestation benign activity itself, and not considering the underlying surface changes of the potential influence. **Figure 10** shows the evaluation diagram of the improvement of water resources utilization efficiency. Afforestation is not only a process of water resources utilization, but also a process of changing the characteristics of the surface and the underlying surface. These changes may significantly affect the hydrological cycle of the basin.

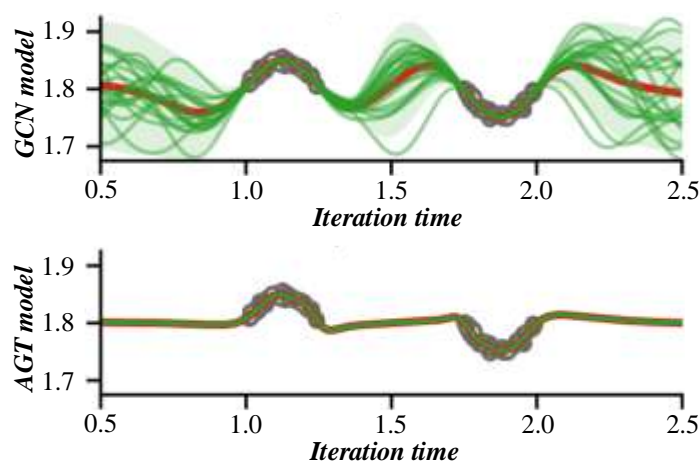


**Figure 10.** Evaluation diagram of water resource utilization efficiency improvement.

The strategic introduction of extensive vegetation, particularly in sloped and hilly terrains, is achieved through a combination of engineering, biological interventions, and methods aimed at conserving water and soil. This initiative focuses on enhancing the coverage rate and strengthening the root systems of plants, which in turn influences the processes of surface runoff and uncontrolled emissions. During drought periods, such as those experienced in the water-scarce Wuding River basin, the importance of these measures becomes particularly pronounced. As illustrated in **Figure 11**, the assessment of the cross-basin water diversion scheme highlights its feasibility. The basin experiences high rates of ineffective evaporation, limited atmospheric precipitation, and minimal surface runoff and deep infiltration. Consequently,

alterations in vegetation cover play a crucial role in shaping the dynamics of the uncontrolled emission process related to evaporation. Positive afforestation efforts can significantly impact not only the total water circulation within the basin but also its spatial and temporal distribution, along with the zonation characteristics. This approach underscores the intricate relationship between vegetation and hydrological processes, revealing that increasing vegetation can mitigate water scarcity challenges while promoting a more resilient ecosystem. By enhancing plant cover, these interventions contribute to improved water retention and reduced runoff, ultimately fostering a more sustainable management of water resources. Moreover, the implications of such changes extend beyond immediate water management, potentially influencing broader ecological dynamics and climate resilience strategies within the region. The integration of these practices is essential for addressing both current and future challenges associated with water scarcity and environmental sustainability in the Wuding River basin.

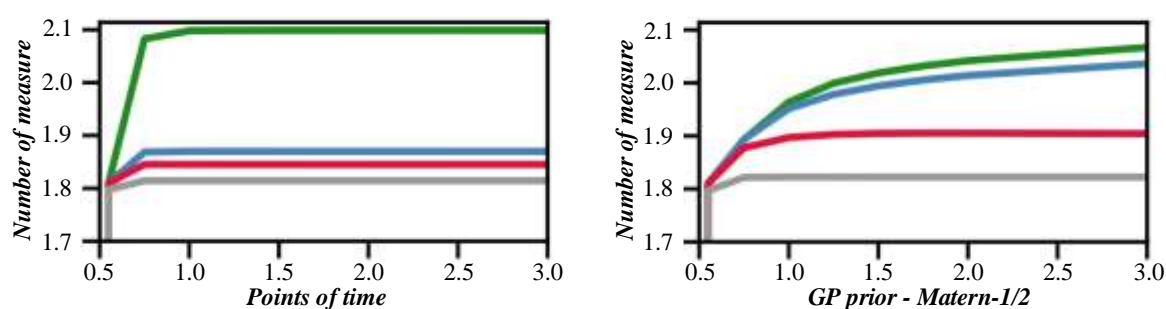


**Figure 11.** Feasibility assessment diagram of the cross-basin water diversion scheme.

## 6. Conclusion

Based on the hydrogeological characteristics and meteorological controllable data of the study area, the deep groundwater flow improvement model is constructed by using the MODFLOW module in GMS (Groundwater Modeling System) software. MODFLOW is a three-dimensional finite difference improvement model developed simulating the flow of deep groundwater, which is widely used in the management and evaluation of deep groundwater resources. In constructing the enhanced model, a comprehensive collection of geological profiles, hydrogeological parameters, and meteorological data from the study area is conducted. This meticulously gathered information is then input into the MODFLOW framework to simulate the fluctuations in flow and water levels of deep groundwater. The simulation results indicate that the enhanced model effectively captures the dynamic changes in groundwater levels within the irrigated regions, demonstrating high levels of simulation accuracy. To achieve optimal coordination between surface water and deep groundwater resources, this study utilizes LinkKitchen software, which facilitates the differential coupling between the modified WEAP and MODFLOW models. LinkKitchen serves as a specialized tool designed for managing the differential coupling of models, enabling the exchange of controllable data and collaborative simulations across various improved frameworks. By employing the WEAP-MODFLOW differential coupling model, this research can simultaneously account for the interactions between surface

water and deep groundwater, allowing for the simulation of more intricate and realistic water resource dynamics.

Upon completing the differential coupling of the enhanced model, parameters will be fine-tuned based on measured flow data from pump stations to ensure the model's precision. The process of determining the rates involves calculating the coefficient of determination, which indicates the degree of correlation between the simulated outputs of the enhanced model and the actual measurements; an  $R^2$  value approaching 1 signifies a superior simulation performance. During both the rate period and validation period, the  $R^2$  value for the modified differential coupling model is approximately 0.98, suggesting exceptional simulation capability. Furthermore, the Nash efficiency coefficient (NSE) assesses the agreement between the simulated and measured values; the closer the NSE value is to 1, the higher the accuracy of the improved model's simulations. The deviation coefficient is used to evaluate the systematic deviation between the simulated values and the measured values of the improved model. The PBIAS value is closer to 0, which indicates that the simulation results of the improved model have no systematic deviation. The PBIAS values of the differential coupling modified model were  $-12\%$  and  $-3.30\%$  during the rate periodic period and validation period, respectively, indicating that the modified model has small bias and reliable simulation results.

**Author contributions:** Conceptualization, ZL and NF; methodology, ZL; software, ZL; validation, ZL, NF; formal analysis, ZL; investigation, ZL; resources, ZL; data curation, ZL; writing—original draft preparation, ZL; writing—review and editing, ZL; visualization, ZL; supervision, ZL; project administration, ZL; funding acquisition, NF. All authors have read and agreed to the published version of the manuscript.

**Ethical approval:** Not applicable.

**Conflict of interest:** The authors declare no conflict of interest.

## References

1. Dai H, Iwasaki T, Shimizu Y. Effect of Sediment Supply on Morphodynamics of Free Alternate Bars: Insights from Hydrograph Boundary Layer. *Water*. 2021; (23): 3437.
2. Wijewardene L, Wu Nai, Giménez GP, Holmboe et al. Epiphyton in Agricultural Streams: Structural Control and Comparison to Epilithon. *Water*. 2021; (23): 3443.
3. Mirzaei M, Yu H, Dehghani A, et al. A Novel Stacked Long Short-Term Memory Approach of Deep Learning for Streamflow Simulation. *Sustainability*. 2021; (23): 13384.
4. Sanz RM, Bladé E, González EF, et al. Interpreting the Manning Roughness Coefficient in Overland Flow Simulations with Coupled Hydrological-Hydraulic Distributed Models. *Water*. 2021; (23): 3433.
5. Gallagher LK, Williams JM, Lazzeri D, et al. Sandtank-ML: An Educational Tool at the Interface of Hydrology and Machine Learning. *Water*. 2021; (23): 3328.
6. Sharannya TM, Venkatesh K, Mudbhatkal A, et al. Effects of land use and climate change on water scarcity in rivers of the Western Ghats of India. *Environmental Monitoring and Assessment*. 2021; (12): 820.
7. Bai Y, Liu M, Yi J, Zhang H. Temporal stability analysis of soil moisture along a coniferous forest hillslope with subtropical monsoon climate in southwest China. *Journal of Mountain Science*. 2021; (11): 2900-2914.
8. Lühr R. Spatial cognition in landscape designations in the area of the Old European. *Hydronymy Lexicographica*. 2021; (1): 59-84.

9. Ndhlovu GZ, Woyessa YE. Evaluation of Streamflow under Climate Change in the Zambezi River Basin of Southern Africa. *Water*. 2021; (21): 3114.
10. Tuheteru EJ, Gautama RS, Kusuma GJ, et al. Water Balance of Pit Lake Development in the Equatorial Region. *Water*. 2021. (21),3106.
11. Lubczonek J, Wlodarczyk SM, Lacka M, Zaniewicz G. Methodology for Developing a Combined Bathymetric and Topographic Surface Model Using Interpolation and Geodata Reduction Techniques. *Remote Sensing*. 2021; (21),4427.
12. Horan R, Rickards NJ, Kaelin A, et al. Extending a Large-Scale Model to Better Represent Water Resources without Increasing the Model's Complexity. *Water*. 2021; (21),3067.
13. Raihan F, Ondrasek G, Islam MS, et al. Combined Impacts of Climate and Land Use Changes on Long-Term Streamflow in the Upper Halda Basin, Bangladesh. *Sustainability*. 2021; (21),12067.
14. De BM, Chidichimo F, Maiolo M, Micallef A. The Impact of Predicted Climate Change on Groundwater Resources in a Mediterranean Archipelago: A Modelling Study of the Maltese Islands. *Water*. 2021; (21),3046.
15. Sirisena TAJG, Maskey S, Bamunawala J, et al. Projected Streamflow and Sediment Supply under Changing Climate to the Coast of the Kalu River Basin in Tropical Sri Lanka over the 21st Century. *Water*. 2021; (21),3031.
16. Meilutytė LD, Akstinas V, Pakhomau A, Nazarenko S, Jurgelėnaitė A. Geographical concerns regarding flood hydrology in the southeastern area of the Baltic Sea basin. *Hydrological Sciences Journal*. 2021; (14),2089-2101.
17. Swarnkar S, Prakash S, Joshi SK, Sinha R. Spatio-temporal rainfall trends in the Ganga River basin over the last century: understanding feedback and hydrological impacts. *Hydrological Sciences Journal*. 2021; (14),2074-2088.
18. Pass FD. Material evidence of folk hydrology in rural Canada: The well auger and dowsing rods of Hamilton “Ham” Brereton. *Water History* (pre-publish). 2021; 1-27.
19. Lousada S, Cabezas J, Castanho RA, Gómez JMN. Hydraulic Planning in Insular Urban Territories: The Case of Madeira Island—Ribeira Brava. *Water*. 2021; (21),2951.
20. Welsh MK, Vidon PG, McMillan SK. Riparian seasonal water quality and greenhouse gas dynamics following stream restoration. *Biogeochemistry*. 2021; (3),453-474.
21. Abernathy, HN, Chandler RB, Crawford DA, et al. Behavioral responses to ecological disturbances influence predation risk for a capital breeder. *Landscape Ecology* (pre-publish). 2021; 1-16.
22. Bokhutlo T, Keppeler FW, Winemiller KO. Seasonal hydrology influences energy channels in food webs of rivers in the lower Okavango Delta. *Environmental Biology of Fishes*. 2021; (10),1303-1319.
23. Lebedeva L, Gustafsson D. Streamflow Changes of Small and Large Rivers in the Aldan River Basin, Eastern Siberia. *Water*. 2021; (19),2747.
24. Hayashi Y, Christie M, Gaillard JC, et al. A transdisciplinary engagement with Australian Aboriginal water and the hydrology of a small bedrock island. *Hydrological Sciences Journal*. 2021; (13),1845-1856.
25. Shishegar S, Ghorbani R, Saad SL, Duchesne S, Pelletier G. Rainfall–runoff modelling using octonion-valued neural networks. *Hydrological Sciences Journal*. 2021; (13),1857-1865.
26. Carmignani JR, Roy AH, Stolarski JT, Richards T. Hydrology of annual winter water level drawdown regimes in recreational lakes of Massachusetts, United States. *Lake and Reservoir Management*. 2021; (4),339-359.
27. Massotti L, Siemes C, March G, Haagmans R, Silvestrin P. Next Generation Gravity Mission Elements of the Mass Change and Geoscience International Constellation: From Orbit Selection to Instrument and Mission Design. *Remote Sensing*. 2021; (19),3935.
28. Yamasaki MSC, Ikehara M, Schiebel R. Two-Tiered Transition of the North Atlantic Surface Hydrology during the Past 1.6 Ma: Multiproxy Evidence from Planktic Foraminifera. *Paleontological Research*. 2021; (4),345-365.
29. Levy J. Episodic basin-scale soil moisture anomalies associated with high relative humidity events in the McMurdo Dry Valleys, Antarctica. *Antarctic Science*. 2021; (5),533-547.
30. Eilander D, van Verseveld W, Yamazaki D, et al. A hydrography upscaling method for scale-invariant parametrization of distributed hydrological models. *Hydrology and Earth System Sciences*. 2021; (9),5287-5313.